Asian Journal of Chemistry; Vol. 38, No. 8 (2026), 2199-2204
ASIAN JOURNAL OF CHEMISTRY
https://doi.org/10.14233/ajchem.2026.36304

Phytochemical Mediated Green Synthesis of Montmorillonite Nanoclay using *Aloe vera* Extract: A Sustainable Approach to Nanomaterial Engineering

AMIT KUMAR BERA[1], VIRENDRA SINGH RANA[2], RAM KARAN SINGH[1], TAPAN KUMAR MANDAL[3] and YASHWANT SINGH BISHT[4,*]

[1]Department of Civil Engineering, ICFAI Tech School, The ICFAI University, Dehradun-248011, India
[2]Department of Mechanical Engineering, ICFAI Tech School, The ICFAI University, Dehradun-248011, India
[3]Department of Chemistry, Bandwan Mahavidyalaya, Purulia-723129, India
[4]Department of Mechanical Engineering, Uttaranchal Institute of Technology, Uttaranchal University, Dehradun-248007, India

*Corresponding author: E-mail: yashwantb3@gmail.com

Received: 24 April 2026 *Accepted*: 27 July 2026 *Published online*: 7 August 2026 AJC-22448

In this study, a phytochemical-mediated green synthesis approach was adopted to fabricate *Aloe vera*-modified montmorillonite nanoclay under mild aqueous conditions. The investigation focused on the ability of naturally occurring phytochemicals, namely polysaccharides, phenolic compounds and flavonoids, to function as surface-functionalising, dispersing, stabilising and intercalating agents for the structural modification of montmorillonite, eliminating the requirement for hazardous chemical modifiers. The synthesised nanoclay was characterised using XRD, FTIR, SEM, particle size distribution analysis and UV-visible spectroscopy to assess its crystal structure, morphology, particle size and surface chemistry. XRD patterns exhibited distinct changes in basal spacing and crystallinity confirmed the successful incorporation of *A. vera*-derived phytochemicals within the layered clay structure. FTIR analysis identified characteristic shifts in absorption bands together with spectral broadening, reflecting strong interactions between the phytochemical constituents and the montmorillonite surface. SEM micrographs depicted a less agglomerated morphology accompanied by partial exfoliation of the clay layers. Particle size distribution analysis placed the majority of particles within the 7-60 nm range, which is consistent with the formation of nanosized material. UV-visible spectra reflected the adsorption of *A. vera* phytochemicals onto the montmorillonite surface, a characteristic associated with successful surface modification through the green synthesis route.

Keywords: Green synthesis, Montmorillonite nanoclay, *Aloe vera* extract, Sustainable nanotechnology.

INTRODUCTION

Nanoparticles possess distinctive physico-chemical properties arising from their high surface-to-volume ratio and quantum confinement effects, making them valuable for applications such as drug delivery, catalysis, optoelectronics and environmental remediation [1-5]. The increasing use of nanomaterials has stimulated the development of sustainable synthesis strategies that minimise environmental and health concerns associated with conventional chemical methods. Conventional synthesis routes, however, often require hazardous chemicals and generate toxic byproducts, creating a need for environmentally benign alternatives.

Green synthesis has emerged as an attractive approach by integrating biological systems into nanomaterial fabrication. Plants, bacteria and fungi have been explored as natural platforms for nanoparticle synthesis due to their ability to facilitate reduction and stabilisation processes [6,7]. Among these, plant-mediated synthesis has received considerable attention owing to its simplicity, cost-effectiveness, scalability and compatibility with eco-friendly processing conditions. Plant extracts contain a wide range of bioactive phytochemicals such as flavonoids, phenolic compounds, terpenoids and polysaccharides, which serve as natural reducing, capping and stabilising agents during nanomaterial formation. Although microbial systems including *Bacillus subtilis* [8], *Penicillium* species [9] and *Fusarium oxysporum* [10], have been employed for nanoparticle synthesis, plant-derived extracts remain more attractive due to their broad availability, straightforward preparation and ease of handling.

Among layered nanomaterials, montmorillonite (MMT) has emerged as an important clay mineral due to its layered

silicate structure and favourable physico-chemical properties. It comprises alternating silica tetrahedral $[SiO_4]^{4-}$ and alumina octahedral $[AlO_3(OH)_3]^{6-}$ sheets, which impart a high aspect ratio, large specific surface area and excellent ion-exchange capacity. These characteristics make MMT an effective nanofiller for polymer composites, improving mechanical strength, thermal stability, flame resistance, barrier performance and gas impermeability [11-15]. The performance of MMT largely depends on the degree of layer exfoliation and surface modification, which govern its compatibility with polymer matrices and other functional materials.

Conventional modification of MMT commonly relies on alkyl ammonium surfactants and other chemical modifiers to expand the interlayer spacing and improve surface compatibility [16]. Although effective, these methods involve hazardous reagents and energy-intensive processing. Plant-derived extracts provide a sustainable alternative by enabling nanoclay modification under mild aqueous conditions without toxic chemicals. Among medicinal plants, *Aloe vera* is recognised for its abundance of polysaccharides, flavonoids, phenolic compounds and saponins, all of which possess reducing, stabilising, capping and surface-active properties [17-19]. These phytochemicals have been extensively employed in the green synthesis of metallic nanoparticles, where they influence the particle size, dispersion and stability [20-22]. Their potential for the direct modification of clay minerals, however, remains comparatively unexplored.

The present study explores a phytochemical-mediated green synthesis of MMT nanoclay using *A. vera* extract as a natural modifying medium. The phytochemical constituents are expected to function simultaneously as surface functionalising, stabilising, dispersing and intercalating agents, promoting nanoscale structural modification under mild aqueous conditions. Structural and surface changes were investigated using X-ray diffraction (XRD), Fourier-transform infrared spectroscopy (FTIR), scanning electron microscopy (SEM), particle size distribution analysis and UV-visible spectroscopy. The findings provide insight into phytochemical assisted clay engineering and establish a sustainable route for preparing functional nanoclay suitable for applications in polymer nanocomposites, environmental remediation, biomedical materials and green construction technologies [23-27].

EXPERIMENTAL

Analytical grade of montmorillonite (MMT) clay was procured from a certified supplier. Fresh leaves of *Aloe barbadensis* Miller were collected from nursery at the ICFAI University, Dehradun, India (Latitude: 30º21′ N, Longitude: 77º52′ E). All chemicals used were of analytical grade and used without further purification. Deionised water was used throughout the experiments.

Preparation of *A. vera* extract: Fresh and healthy *A. vera* leaves were washed thoroughly with distilled water to remove surface contaminants. The outer green rind was peeled and the inner gel was carefully extracted. The gel was then homogenised using a sterile blender and filtered through muslin cloth followed by Whatman grade 1 filter paper to remove particulate matter. The filtrate (clear extract) was stored at 4 ºC and used within 24 h for synthesis purposes.

Pre-treatment of MMT clay: The raw MMT clay was pre-treated to remove organic impurities. The clay was dispersed in deionised water (1:10 w/v) and stirred for 6 h at room temperature. The suspension was then centrifuged at 4000 rpm for 15 min. The pellet was washed several times with deionised water until neutral pH was achieved and dried at 60 ºC in a hot air oven for 12 h.

Green Synthesis of MMT based nanoclay: A pre-treated MMT sample (5 g) was dispersed in 100 mL of deionised water and sonicated for 30 min to obtain a homogeneous suspension. Freshly prepared *A. vera* extract (50 mL) was then introduced dropwise under continuous magnetic stirring. The suspension was stirred at ambient temperature for 24 h to promote interaction between the clay surface and the phytochemical constituents of the extract. Polysaccharides, phenolic compounds, flavonoids and other oxygen-containing biomolecules present in *A. vera* extract. Adsorption of these phytochemicals onto the MMT surface modified the interlayer environment, promoted partial exfoliation of the clay platelets and reduced particle agglomeration, leading to the formation of nanostructured MMT. The suspension was centrifuged at 6000 rpm for 20 min, followed by repeated washing with deionised water to remove loosely bound phytochemicals. The filtered solid was dried at 60 ºC and finely ground.

Characterisation: The green-synthesised MMT nanoclay was characterised using analytical techniques to examine its structural, morphological, optical and surface properties. X-ray diffraction (XRD) analysis was performed using a Bruker D-8 diffractometer with Cu*K*α radiation (λ = 1.54 Å) operating at 40 mA. Diffraction patterns were recorded over a 2θ range of 5-90º at a scanning rate of 2º/mim and analysed with the JCPDS/PDF database for phase identification and structural evaluation. Surface morphology and particle characteristics were examined using a QUANTA 200 FEG scanning electron microscope (SEM) after sputter coating the samples with a conductive layer. Fourier-transform infrared (FTIR) spectroscopy was carried out in the 4000-400 cm^{-1} region to identify the functional groups and examine interactions between MMT and *A. vera* phytochemicals. UV-visible spectroscopy was recorded over the wavelength range of 200-700 nm to investigate optical absorption behaviour associated with phytochemical adsorption and surface modification of the MMT nanoclay.

RESULTS AND DISCUSSION

A green synthesis route employing *Aloe vera* extract was developed for the preparation of MMT nanoclay under mild aqueous conditions. Phytochemicals, primarily phenolics, flavonoids and polysaccharides, functioned as natural surface-functionalising, dispersing, stabilising and intercalating agents. Their interaction with the layered MMT structure through ion exchange, coordination interactions and hydrogen bonding modified the surface, expanded the interlayer spacing and promoted partial exfoliation into nanoscale platelets.

Particle size distribution analysis: The particle size distribution of the green synthesised MMT nanoclay is shown in Fig. 1. The particles were primarily distributed within the 7-60 nm range, with the highest volume fraction centred

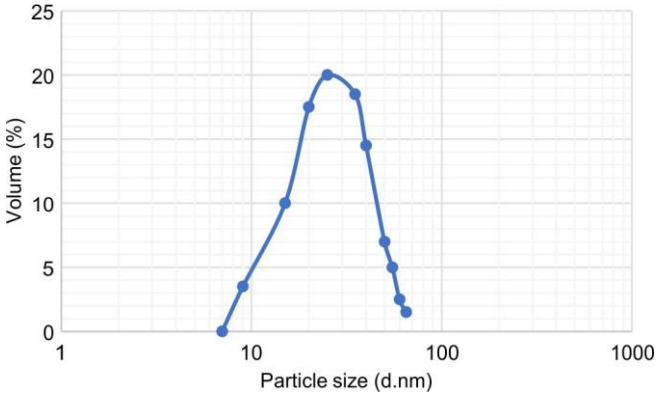

Fig. 1. Particle size distribution of *Aloe vera*-mediated MMT nanoclay

between 25 and 35 nm, reflecting a relatively narrow size distribution. Particle populations exceeding 100 nm were negligible, consistent with effective phytochemical-assisted size reduction and suppression of particle agglomeration. According to the internationally accepted definition, materials possessing at least one external dimension below 100 nm are classified as nanomaterials. The measured particle size distribution satisfies this criterion, establishing the successful formation of MMT nanoclay.

XRD: To examine the structural modification of MMT following phytochemical treatment, the XRD pattern of the synthesised nanoclay was compared with that of pristine MMT (Fig. 2). The untreated clay exhibited the characteristic basal reflection of MMT at 2θ = 6.68º, together with diffraction peaks attributed to quartz and calcite impurities. Treatment with *A. vera* extract altered both the position and intensity of the diffraction peaks. The basal reflection shifted from 6.68º to 10.28º, is attributed to the changes in the interlayer environment arising from interactions between the clay layers and *A. vera* phytochemicals. Such peaks displacement are attributed due to the ion-exchange, interlayer rearrangement, partial dehydration of exchangeable cations and surface functionalisation of layered silicates.

The modified nanoclay exhibited additional reflections at 2θ values of 25.28º, 27.68º, 36.94º, 37.80º, 38.57º, 55.06º and 62.12º. The diffraction patterns exhibit broader peaks and lower intensities, which reveals reduced crystallinity, higher lattice disorder and partial exfoliation of the layered structure after phytochemical treatment. Quartz reflections remained essentially unchanged, because the associated mineral impurities were largely unaffected, whereas the structural changes were confined to the MMT phase. The observed diffraction behaviour is consistent with adsorption of phytochemical constituents onto the clay surface, followed by hydrogen bonding, ion-exchange and interlayer interactions that modified the layered architecture of MMT [28].

SEM: The SEM micrographs of pristine MMT clay and *A. vera*-mediated synthesised nanoclay are shown in Fig. 3a-c. The untreated MMT clay exhibits relatively large, compact and highly aggregated platelet-like particles with a characteristic layered morphology, as observed at magnifications of 2500x and 6000x. The clay platelets appear densely stacked with irregular agglomerates, which is typical of naturally occurring MMT resulting from strong interparticle interactions and layer stacking.

Following treatment with *A. vera* extract, a distinct morphological transformation is observed. The synthesised material exhibits smaller, thinner and more uniformly dispersed platelet like particles with reduced agglomeration compared with the pristine clay. Interaction between the phytochemicals and MMT disrupted the stacked clay layers, leading to the partial exfoliation, fragmentation and improved particle dispersion. The observed reduction in particle aggregation is attributed to the adsorption of phytochemical molecules on the clay surface, which likely reduced interparticle attractive forces during the green synthesis process. This observations are further supported by the XRD analysis, which revealed changes

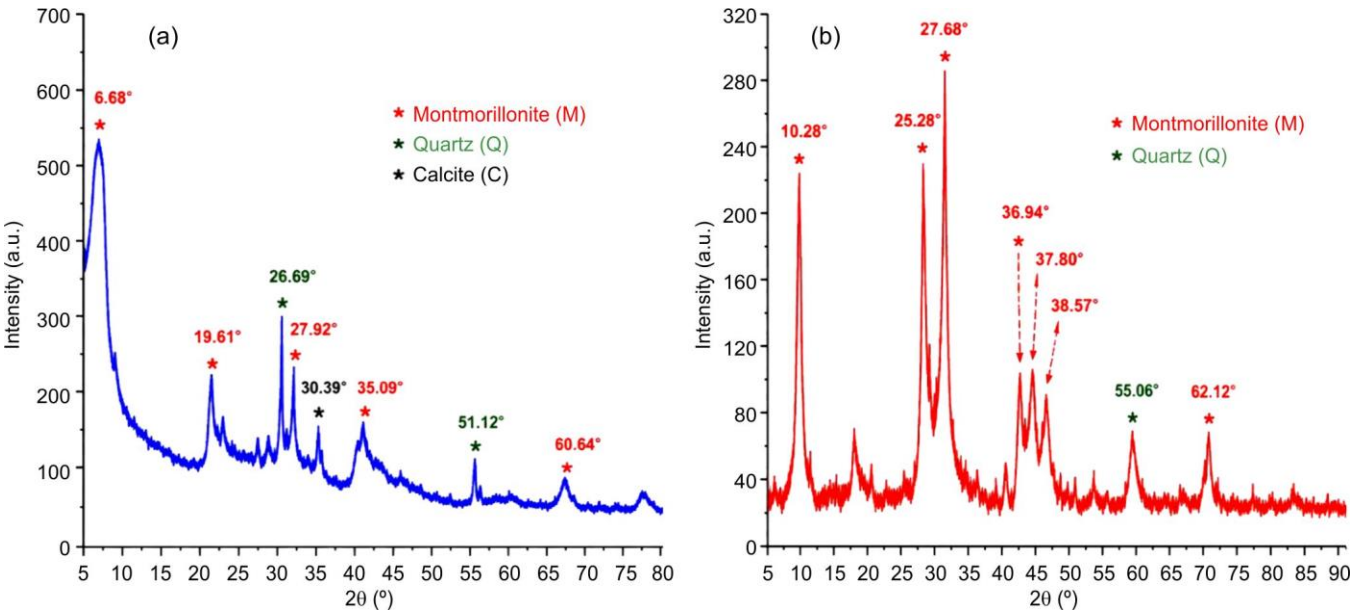

Fig. 2. Comparative XRD patterns of (a) pristine MMT clay and (b) *Aloe vera*-mediated MMT nanoclay, illustrating changes in diffraction peak positions, intensities and crystallinity following phytochemical treatment

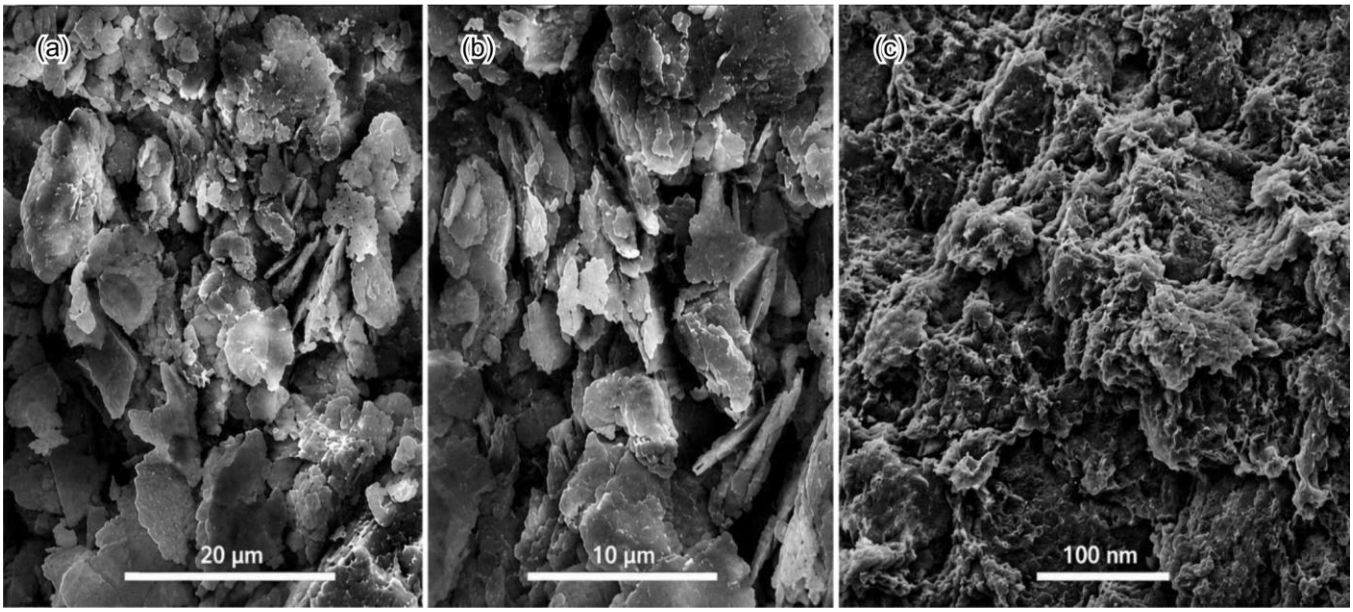

Fig. 3. Scanning electron microscopy (SEM) micrographs of (a) pristine MMT clay at 2500× magnification, (b) pristine MMT clay at 6000× magnification and (c) phytochemically synthesised MMT nanoclay using *Aloe vera* extract

in diffraction peak position, peak broadening and reduced crystallinity following phytochemical treatment.

FTIR: Fig. 4 compares the FTIR spectra of pristine MMT and green-mediated MMT nanoclay. The spectrum of pristine MMT contains the characteristic absorption bands of layered aluminosilicates, comprising Si–O stretching at 1045 cm^{-1}, Al–Al–OH bending at 920 cm^{-1}, Si–O–Al vibrations within the 881-797 cm^{-1} region and structural O–H stretching near 3643 cm^{-1}. These absorption bands correspond to the typical mineralogical structure of MMT.

Treatment with *A. vera* extract altered both the position and profile of several absorption bands. For example, the peak displacements from 1045 to 1035 cm^{-1} for the Si–O stretching vibration and from 920 to 915 cm^{-1} for the Al–OH–Al deformation band are characteristic of modifications in the local chemical environment of the silicate framework. Such spectral variations are the characteristic of interactions between phytochemical constituents and the clay surface through hydrogen bonding, electrostatic attraction and surface functionalisation.

The sharp structural O–H band of pristine MMT at approximately 3643 cm^{-1} was replaced by a broad absorption envelope centred near 3440 cm^{-1}, together with bands at 3623 and 3697 cm^{-1}. This broadening is attributed to hydroxyl-rich

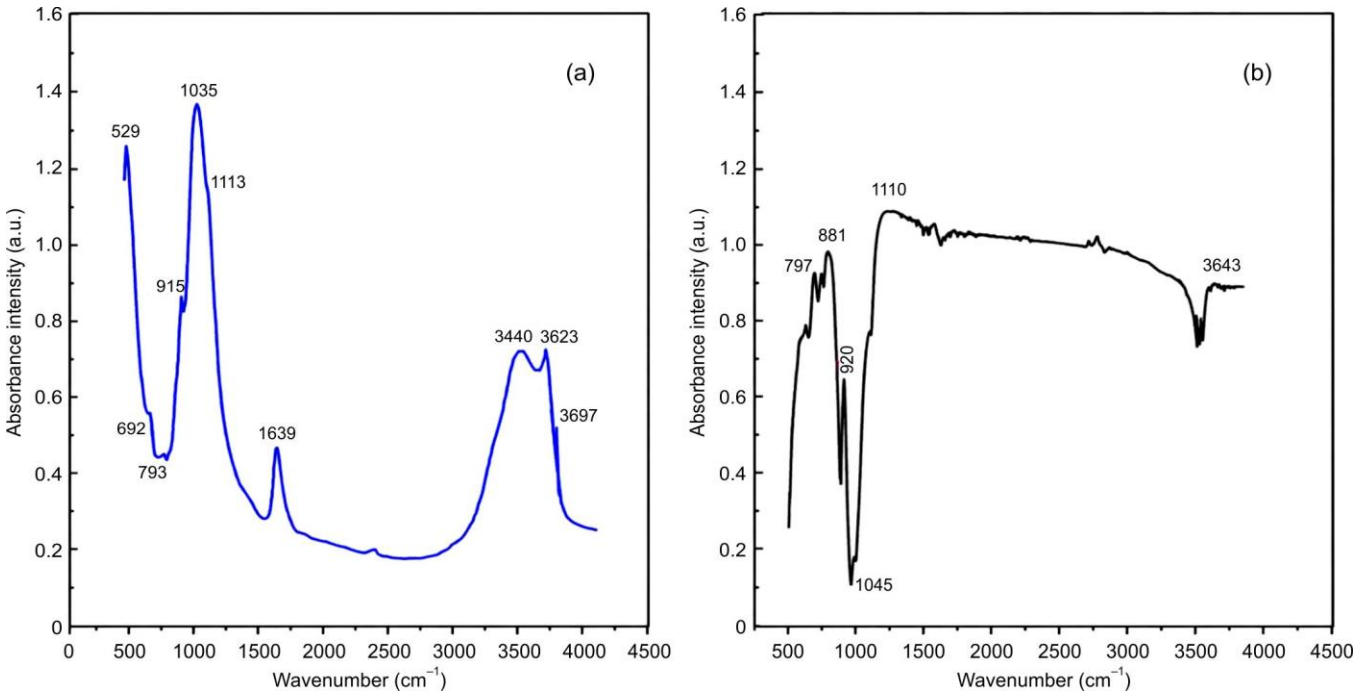

Fig. 4. FTIR spectra of (a) pristine MMT clay and (b) *Aloe vera*-mediated synthesised MMT nanoclay

phytochemicals adsorbed onto the clay surface and modifications in the hydrogen-bonding environment. An absorption band at 1639 cm^{-1}, assigned to H–O–H bending vibrations and oxygen-containing organic functional groups, further shows the presence of *A. vera* phytochemicals associated with the MMT structure [29].

UV-Vis spectroscopy: The UV-Vis absorption spectrum of the green-mediated MMT nanoclay is shown in Fig. 5. A prominent absorption maximum occurs at approximately 320 nm, followed by a broad absorption band extending into the visible region with a shoulder near 433 nm. The absorption at 320 nm originates from electronic transitions of oxygen-containing phytochemicals such as phenolic compounds, flavonoids, anthraquinones and polysaccharide-derived functional groups, adsorbed onto the MMT surface during synthesis. The broad absorption between 330 and 550 nm, together with the shoulder at 433 nm, is characteristic of interactions between phytochemical ligands and hydroxylated aluminosilicate layers, involving ligand-to-metal charge-transfer processes associated with structural Al^{3+}, Mg^{2+} and Fe^{3+} ions, together with light scattering from the modified clay particles. Since MMT is a layered aluminosilicate rather than a semiconductor, the observed absorption features are attributed to phytochemical adsorption and surface functionalisation rather than quantum confinement or other nanoscale electronic effects.

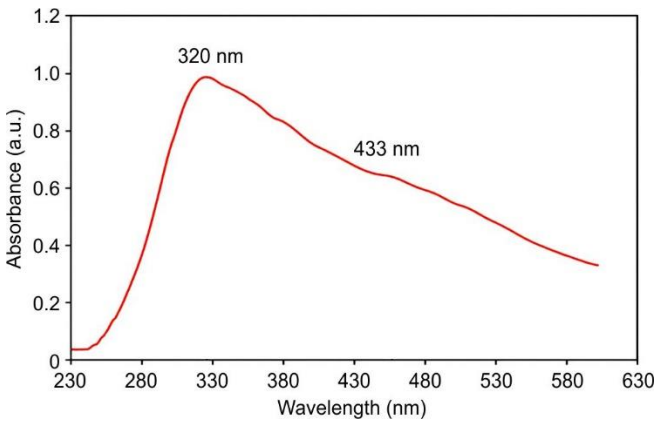

Fig. 5. UV-visible absorption spectrum of phytochemical mediated synthesised MMT nanoclay

Mechanism of phytochemical mediated functionalisation of MMT nanoclay: The functionalisation of MMT by phytochemicals proceeds through a combination of coordination interactions, ion- exchange, hydrogen bonding and intercalation mechanisms. The pristine MMT structure, $(Na,Ca)_{0.33}(Al,Mg)_2Si_4O_{10}(OH)_2{\cdot}nH_2O$ contains exchangeable interlayer cations (Na^+/Ca^{2+}), which play a crucial role in facilitating interactions with bioactive molecules.

Phenolic compounds undergo deprotonation under suitable conditions to form phenolate ions ($Ph–O^-$), which replace interlayer Na^+ ions *via* ion-exchange processes, leading to the formation of organically modified clay, MMT–$(O–Ph)_x$. Similarly, flavonoids, possessing multiple hydroxylated aromatic rings, interact more strongly with the clay surface through both ion-exchange and multidentate coordination with octahedral Al^{3+} centres, resulting in stable hybrid structures, MMT–$(O–Ar)_x$. In contrast, polysaccharides primarily interact through hydrogen bonding between their hydroxyl groups and surface silanol (≡Si–OH) groups of MMT, along with partial intercalation into the interlayer galleries.

These interactions promote expansion of the basal spacing (*d*-spacing), weaken interlayer forces and facilitate exfoliation of the layered structure into nanoscale platelets. The modified material can be represented as phytochemical-functionalised nanoclay MMT–$(organic)_x$, $[(Na,Ca)_{0.33}(Al,Mg)_2Si_4O_{10}(OH)_2{\cdot}nH_2O{\cdot}(O–R)_x]$ exhibiting enhanced surface reactivity, dispersion stability and potential applicability in advanced material systems. (where x represents the total degree of surface functionalisation and R denotes the phytochemical moieties phenolic (Ph), flavonoid (Ar) and polysaccharide-derived functional groups incorporated *via* ion-exchange, coordination and hydrogen bonding).

Conclusion

A green synthesis route employing *A. vera* extract was developed for the phytochemical-mediated modification of MMT under mild aqueous conditions. Naturally occurring phytochemicals functioned as surface-functionalising, dispersing, stabilising and intercalating agents, eliminating the need for conventional chemical modifiers. Interactions involving ion exchange, hydrogen bonding, coordination, and adsorption altered the interlayer environment, promoted partial exfoliation and improved dispersion of the clay particles. The proposed modification mechanism was supported by characterisation techniques. XRD identified changes in basal reflection and crystallinity associated with structural modification of MMT. FTIR spectra exhibited peak displacements and hydroxyl band broadening arising from interactions between *A. vera* phytochemicals and the clay surface. SEM micrographs showed a less agglomerated morphology accompanied by partial exfoliation of the layered structure. Particle size analysis placed most particles within the 7-60 nm range, meeting the accepted size criterion for nanomaterials. The UV-Vis spectrum contained absorption bands attributed to *A. vera* phytochemicals adsorbed on the MMT surface, consistent with surface functionalisation of the clay. The modified MMT retained its layered aluminosilicate framework while acquiring phytochemical-derived surface functionalities and nanoscale characteristics.

ACKNOWLEDGEMENTS

The authors gratefully acknowledge the support and facilities provided by the Indian Institute of Technology, Roorkee (IITR) and the Council of Scientific and Industrial Research-Indian Institute of Petroleum (CSIR-IIP), Dehradun, for enabling the experimental work and assisting in data analysis. The authors also extend their sincere appreciation to ICFAI Tech School, The ICFAI University, Dehradun, for offering the necessary institutional support and a conducive academic environment that contributed to the successful completion of this research.

CONFLICT OF INTEREST

The authors declare that there is no conflict of interests regarding the publication of this article.

DECLARATION OF AI-ASSISTED TECHNOLOGIES

During the preparation of this manuscript, the authors used an AI-assisted tool(s) to improve the language and no data, results or scientific conclusions were generated by AI. All analyses, interpretations and conclusions are the authors' own. The authors reviewed and edited the content and take full responsibility for the published work.

REFERENCES

1. B. Abera, G. Kahsay, T. Negussie and G. Mebratie, *Results Chem.*, **27**, 103450 (2026); https://doi.org/10.1016/j.rechem.2026.103450
2. M. Abdullah, M. Obayedullah, M.S.I. Shuvo, M.A. Khair, D. Hossain, and M.N. Islam, *Results Surf. Interfaces*, **21**, 100635 (2025); https://doi.org/10.1016/j.rsurfi.2025.100635
3. N. Baig, I. Kammakakam and W. Falath, *Mater. Adv.*, **2**, 1821 (2021); https://doi.org/10.1039/D0MA00807A
4. T.A. Saleh, *Environ. Technol. Innov.*, **20**, 101067 (2020); https://doi.org/10.1016/j.eti.2020.101067
5. S. Bakand, A. Hayes and F. Dechsakulthorn, *Inhal. Toxicol.*, **24**, 125 (2012); https://doi.org/10.3109/08958378.2010.642021
6. A. Lateef, S.A. Ojo and J.A. Elegbede, *Nanotechnol. Rev.*, **5**, 6 (2016); https://doi.org/10.1515/NTREV-2016-0049/HTML
7. H. Duan, D. Wang and Y. Li, *Chem. Soc. Rev.*, **44**, 5778 (2015); https://doi.org/10.1039/C4CS00363B
8. P.A. Sundaram, R. Augustine and M. Kannan, *Biotechnol. Bioprocess Eng.*, **17**, 835 (2012); https://doi.org/10.1007/s12257-011-0582-9
9. L. Du, L. Xian and J.-X. Feng, *J. Nanopart. Res.*, **13**, 921 (2011); https://doi.org/10.1007/s11051-010-0165-2
10. J.C. Masini and G. Abate, *Minerals*, **11**, 1282 (2021); https://doi.org/10.3390/min11111282
11. L. Perelomov, S. Mandzhieva, T. Minkina, Y. Atroshchenko, T. Bauer, I. Perelomova, D. Pinsky and A. Barakhov, *Minerals*, **11**, 707 (2021); https://doi.org/10.3390/min11070707
12. T. Undabeytia, U. Shuali, S. Nir and B. Rubin, *Minerals*, **11**, 9 (2020); https://doi.org/10.3390/min11010009
13. A. Jacquet, D.L. Geatches, S.J. Clark and H.C. Greenwell, *Minerals*, **8**, 130 (2018); https://doi.org/10.3390/min8040130
14. G. Lazorenko, A. Kasprzhitskii and V. Yavna, *Minerals*, **10**, 732 (2020); https://doi.org/10.3390/min10090732
15. H. Shokrani, A. Shokrani, M. Jouyandeh, F. Seidi, F. Gholami, S. Kar, M.T. Munir, D. Kowalkowska-Zedler, P. Zarrintaj, N. Rabiee and M.R. Saeb, *ACS Appl. Bio Mater.*, **5**, 2107 (2022); https://doi.org/10.1021/acsabm.2c00313
16. A. Barra, C. Nunes, E. Ruiz-Hitzky and P. Ferreira, *Int. J. Mol. Sci.*, **23**, 1848 (2022); https://doi.org/10.3390/ijms23031848
17. R. Pandey and V. Vishwakarma, *Discov. Chem.*, **3**, 122 (2026); https://doi.org/10.1007/s44371-026-00527-6
18. C.I. Idumah, U. Okonkwo and C. Obele, *Clean. Mater.*, **4**, 100071 (2022); https://doi.org/10.1016/j.clema.2022.100071
19. A. Paul, R. Augustine, A. Hasan, A.A. Zahid, S. Thomas, C. Agatemor and K. Ghosal, *J. Drug Deliv. Sci. Technol.*, **72**, 103380 (2022); https://doi.org/10.1016/j.jddst.2022.103380
20. R.R. Palem, K.M. Rao, G. Shimoga, R.G. Saratale, S.K. Shinde, G.S. Ghodake and S.-H. Lee, *Int. J. Biol. Macromol.*, **178**, 464 (2021); https://doi.org/10.1016/j.ijbiomac.2021.02.195
21. Y. Wu, J. Wu, C. Mei, R. Yang, W. He, X. Li, L. Cai, M. Guo, J. Li and C. Xia, *Environ. Res.*, **213**, 113724 (2022); https://doi.org/10.1016/j.envres.2022.113724
22. M.A.F. Calesco, A. Watanuki Filho, M.R. Moura and F.A. Aouada, *Ceramica*, **68**, 97 (2022); https://doi.org/10.1590/0366-69132022683853161
23. H. Oliver-Ortega, V. Vandemoortele, A. Bala, F. Julian, J.A. Méndez and F.X. Espinach, *Polymers*, **13**, 16 (2021); https://doi.org/10.3390/polym13162741
24. P. Chaiwutthinan, N. Phutfak and A. Larpkasemsuk, *J. Appl. Polym. Sci.*, **133**, 20 (2021); https://doi.org/10.1002/APP.50443
25. R. Yadav, R. Purwar and U. Bose, *Mater. Today Proc.*, **45**, 4998 (2021); https://doi.org/10.1016/j.matpr.2021.01.424
26. J. Miedzianowska, M. Masłowski, P. Rybiński and K. Strzelec, *Polymers*, **13**, 799 (2021); https://doi.org/10.3390/polym13050799
27. S.A. Hosseini, S. Daneshvar e Asl, M. Vossoughi, A. Simchi and M. Sadrzadeh, *ACS Omega*, **6**, 10816 (2021); https://doi.org/10.1021/acsomega.1c00480
28. M. Paredes-Laverde, D.F. Montaño and R.A. Torres-Palma, *Water*, **15**, 1046 (2023); https://doi.org/10.3390/w15061046
29. F.R. Isfahani, H. Tavanai and M. Morshed, *Fibers Polym.*, **18**, 264 (2017); https://doi.org/10.1007/s12221-017-6954-9